Electronic Supplementary Information

Tailoring long-range superlattice chirality in the molecular self-assemblies via weak fluorine-mediated interactions

Mykola Telychko[†a], Lulu Wang[†a], Chia-Hsiu Hsu[†b], Guangwu Li[†a], Xinnan Peng[a], Shaotang Song[a], Jie Su[a], Feng-Chuan Chuang*[b], Jishan Wu*[a], Ming Wah Wong*[a] and Jiong Lu*[a,c]

[a] Department of Chemistry, National University of Singapore, 3 Science Drive 3, Singapore 117543, Singapore

[b] Department of Physics, National Sun Yat-Sen University, Kaohsiung 80424, Taiwan; Physics Division, National Center for Theoretical Sciences, Taipei, 10617 Taiwan

[c] Centre for Advanced 2D Materials (CA2DM), National University of Singapore, 6 Science Drive 2, Singapore 117546, Singapore

† These authors contributed equally to this work.

* Corresponding authors: Email: chmluj@nus.edu.sg (J. Lu); chmwmw@nus.edu.sg (M. W. Wong); chmwuj@nus.edu.sg (J. Wu); fchuang@mail.nsysu.edu.tw (F.C. Chuang);

Table of Contents

1. Additional STM images of HPB and F-HPB self-assemblies

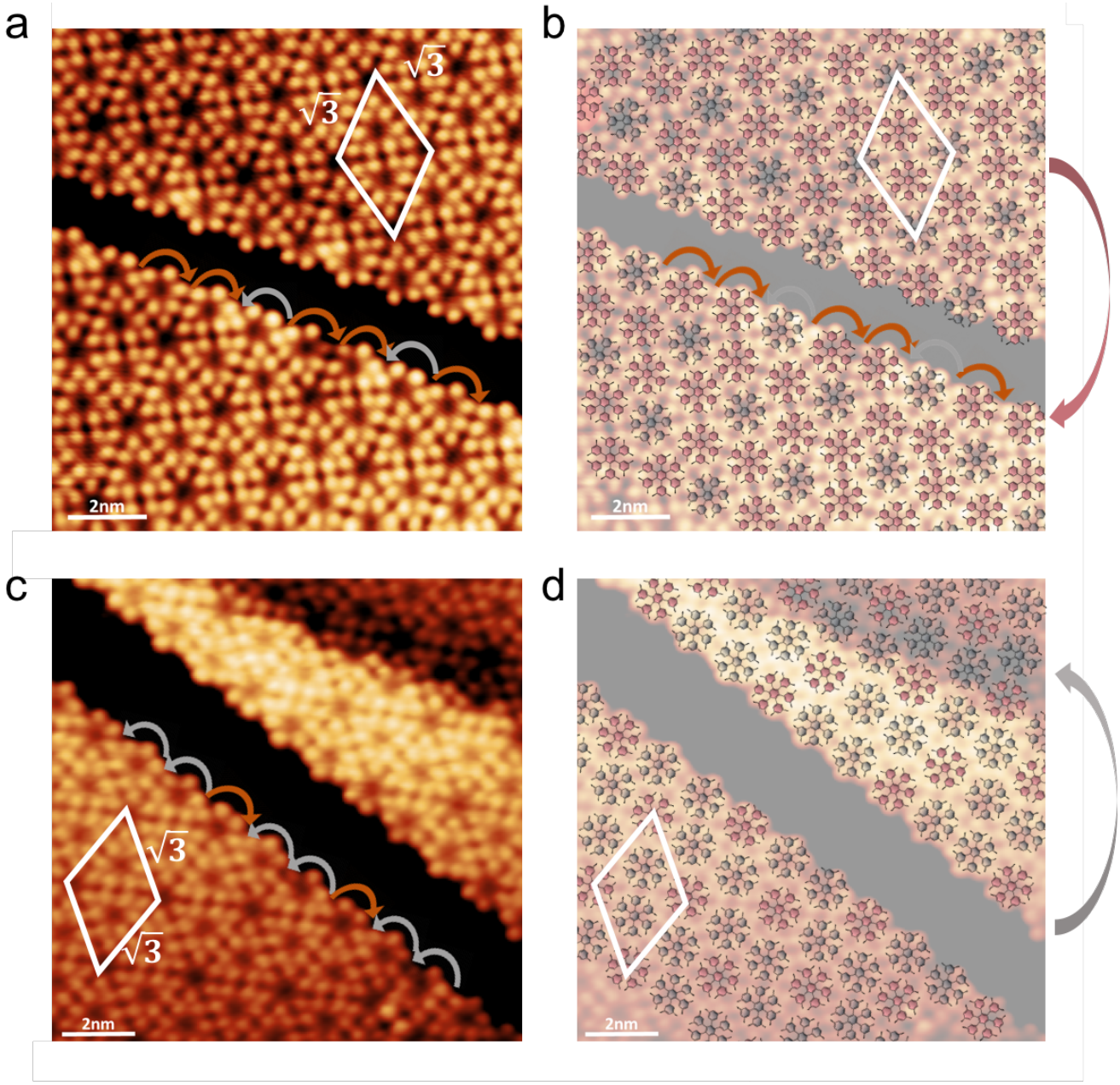

Fig. S1. Additional STM images of HPB self-assemblies. (a) STM image of the HPB assembly with net L- long-range superlattice chirality. (b) Image in panel a superimposed with chemical structures of HPB molecule. (c) STM image of the HPB assembly with net R- long-range superlattice chirality. (d) Image in panel c superimposed with chemical structures of HPB molecule. Grey and pink molecular structures denote L- handed and R- handed HPB enantiomers, respectively.

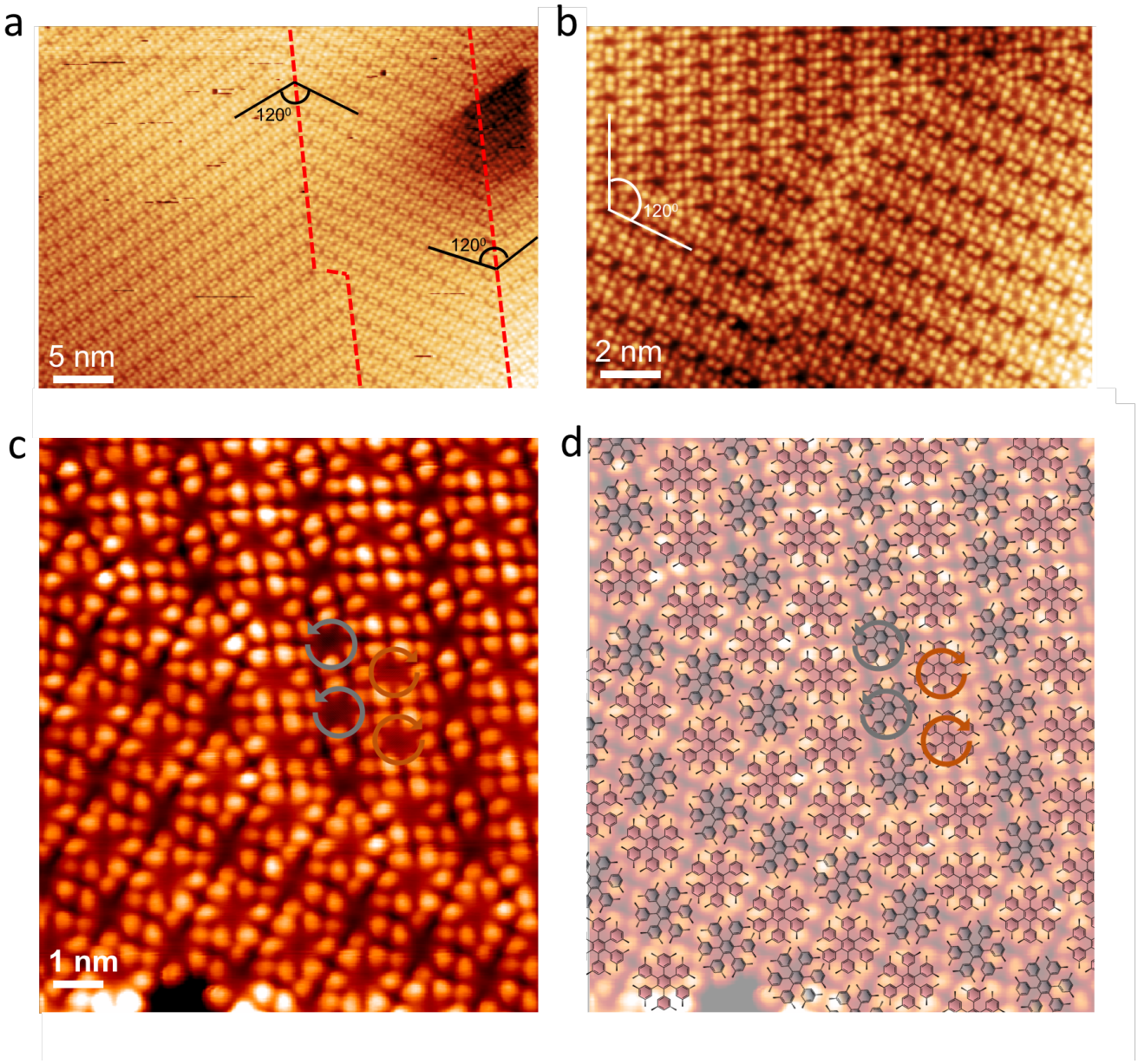

Figure S2. Additional STM images of F-HPB self-assemblies. (a) Large-scale image of F-HPB assembly shows a coexistence of multiple 2×1domains and domain boundaries. (b) High-resolution image of F-HPB assembly reveals the presence of multiple 2×1 domains co-existed with the $\sqrt{3} \times \sqrt{3}$ phase. (c) High-resolution image highlights the L- and R- enantiomers. (d) Image in panel c superimposed with chemical structures of F-HPB molecules. Grey and pink molecular structures denote L- handed and R- handed F-HPB enantiomers, respectively.

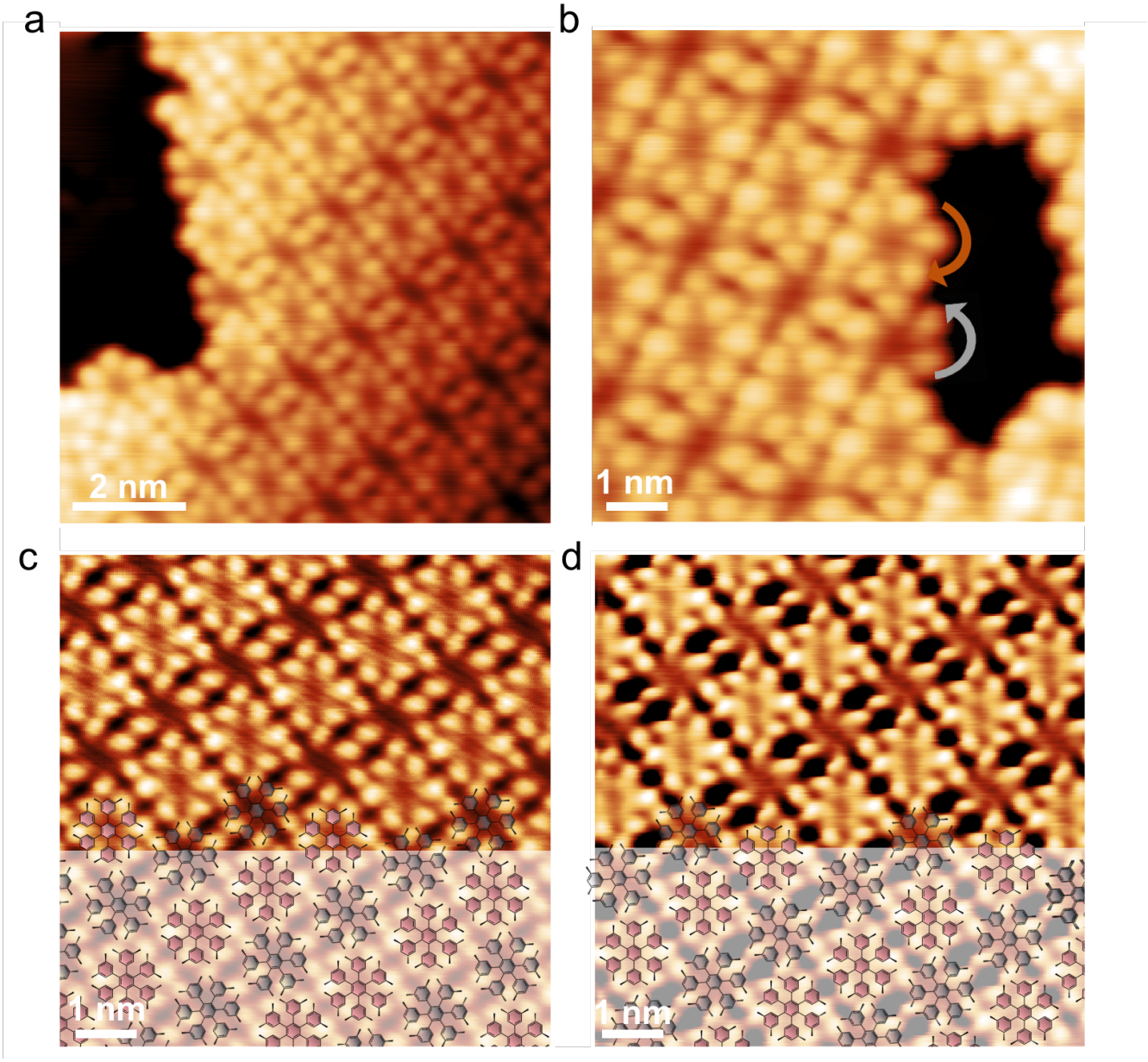

Figure S3. Additional STM images of F-HPB self-assembly. (a, b) STM Images of self-assembled monolayer F-HPB islands with edges. (c, d) STM images acquired at different tunneling parameters: *Vs* = 1V, *I* = 0.5 nA (panel (c)) and *Vs* = 0.1V, *I* = 1 nA (panel (d)). Grey and pink molecular structures denote L- handed and R- handed F-HPB enantiomers, respectively.

2. Energies of the HPB and F-HPB structures

Table S1. The energy per molecule of HPB/FHPB $\sqrt{3} \times \sqrt{3}$ and 2×1 superstructures.

Opt. single point energy (eV)	$\sqrt{3} \times \sqrt{3}$	2×1
HPB	-690.9654	-690.8591
F-HPB	-692.8607	-692.9254

Table S2. Cohesive energies of the heterochiral and homochiral enantiomers is HPB $\sqrt{3} \times \sqrt{3}$ and F-HPB 2×1 structure

Unit cell	HPB		F-HPB		
	heterochiral	homochiral	homochiral-L	heterochiral	homochiral-R
Cohesive energy (kJ/mol)	-48.91	-29.3	-22.6	-43.39	-19.1
BSSE corrected (kJ/mol)	-45.77	-26.4	-19.8	-38.45	-16.8

3. Charge density difference plots of the HPB and F-HPB assemblies

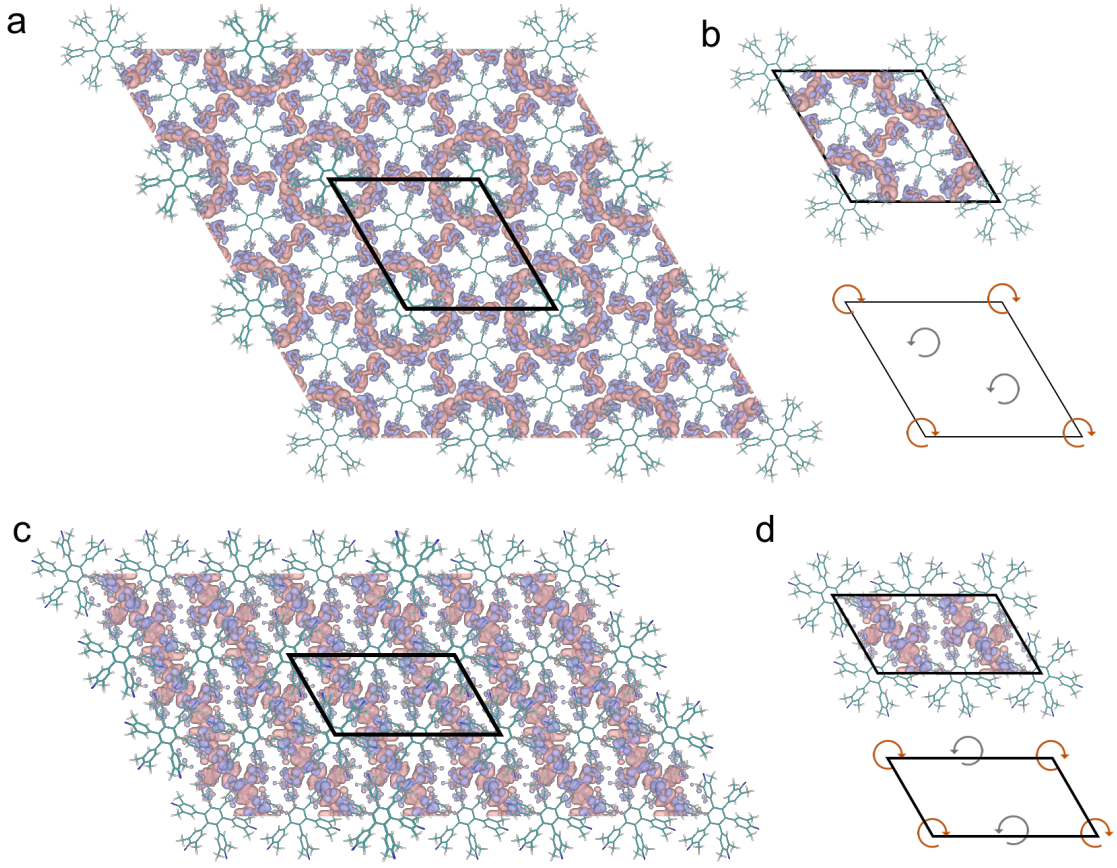

Figure S4. Charge density difference plots of HPB and F-HPB assemblies. (a, b) Charge density difference (CDD) plots (panel (a)) and zoom-in image (panel (b)) of one unit cell the HPB assembly and (c, d) charge density difference (panel (c)) and zoom-in image of one unit cell (panel (d)) of the F-HPB assembly. The depletion and accumulation of negative charge is denoted by pink and purple color, respectively. Both CDD plots were generated at an isosurface of 0.0001e/Å^3

4. Additional NCI calculations of HPB and F-HPB assemblies

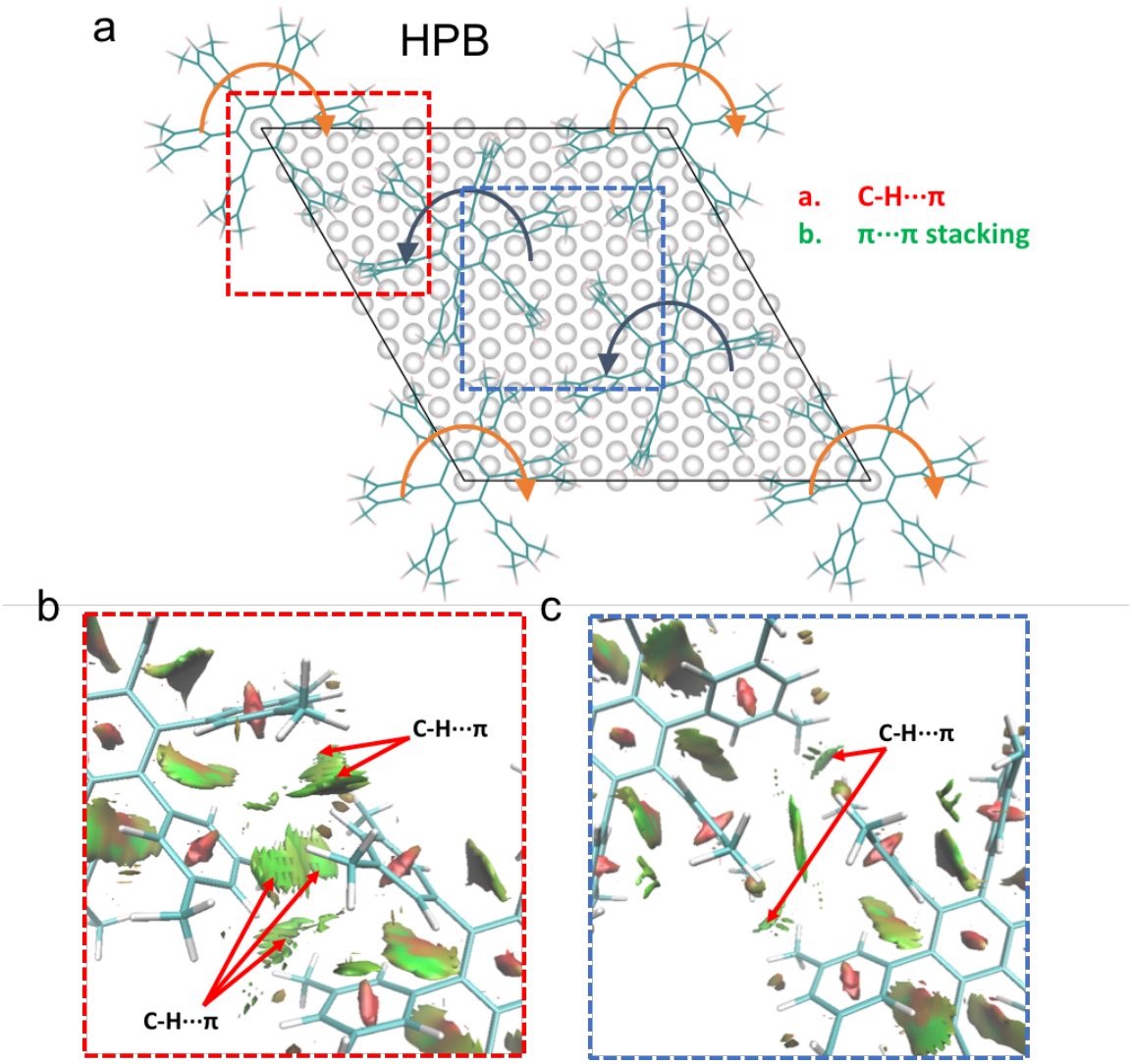

Fig. S5. Weak non-covalent interactions in HPB assembly. (a) DFT-relaxed $\sqrt{3} \times \sqrt{3}$ elementary unit cell of the HPB assembly. (b, c) NCI plots of magnified view of the area marked by red (panel (b)) and red rectangle (panel (c)), revealing multiple weak C-H···π interactions between heterochiral HPB enantiomers (denoted as a_1-a_5). The weak NCIs are represented by the discs. The color of the discs is ranging from blue (strong attraction) to red (strong repulsion). The results are consistent with the AIM results (see Table S3).

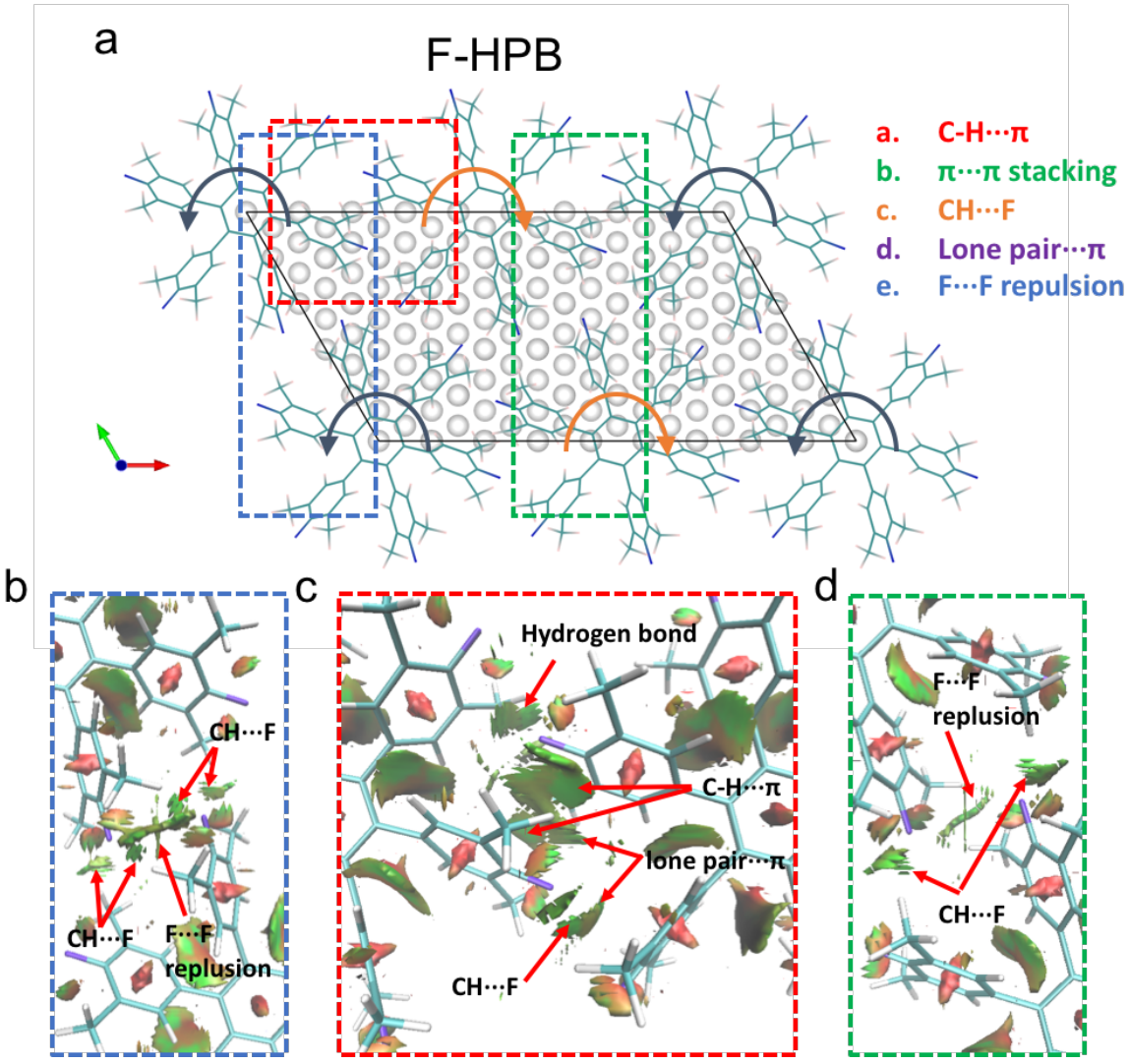

Fig. S6. Weak non-covalent interactions in F-HPB assembly. (a) DFT-relaxed 2 × 1 elementary unit cell of the F-HPB assembly. (b, c, d) NCI plots of magnified view of the area marked by blue (panel b), red (panel c) and green (panel d) rectangle reveals a set of weak NCIs between heterochiral F-HPB enantiomers including C-H··· π (denoted as a_1, a_2), C-H···F (b_1-b_3) and F Lone pair···π (c_1, c_2). The NCI results are consistent with the AIM results (see Table S4).

Table S3. Calculated topological properties of the electron density for the intermolecular interaction for HPB $\sqrt{3} \times \sqrt{3}$ structure

s

HPB					
heterochiral			homochiral		
BCP	ρ (r) (a.u.)	Laplacian ρ (r) (a.u.)	BCP	ρ (r) (a.u.)	Laplacian ρ (r) (a.u.)
a1	0.00194	0.00571	a1	0.00075	0.00239
a2	0.00297	0.00878	a2	0.00075	0.00238
a3	0.00432	0.01278	b1	0.00206	0.00531
a4	0.00295	0.00868			
a5	0.00189	0.00556			

Table S4. Calculated topological properties of the electron density for the intermolecular interaction for F-HPB 2×1 structure

F-HPB								
homochiral-L			heterochiral			homochiral-R		
BCP	ρ (r) (a.u.)	Laplacian ρ (r) (a.u.)	BCP	ρ (r) (a.u.)	Laplacian ρ (r) (a.u.)	BCP	ρ (r) (a.u.)	Laplacian ρ (r) (a.u.)
c1	0.00372	0.01791	a1	0.00673	0.0215	c1	0.00531	0.0243
c2	0.00605	0.02721	a2	0.00699	0.02188	c2	0.00526	0.02413
c3	0.00611	0.02746	c1	0.00748	0.03351	e1	0.00104	0.00715
c4	0.00363	0.01748	c2	0.00635	0.02924			
e1	0.00266	0.01678	d1	0.00278	0.01211			
			d2	0.0052	0.02297			

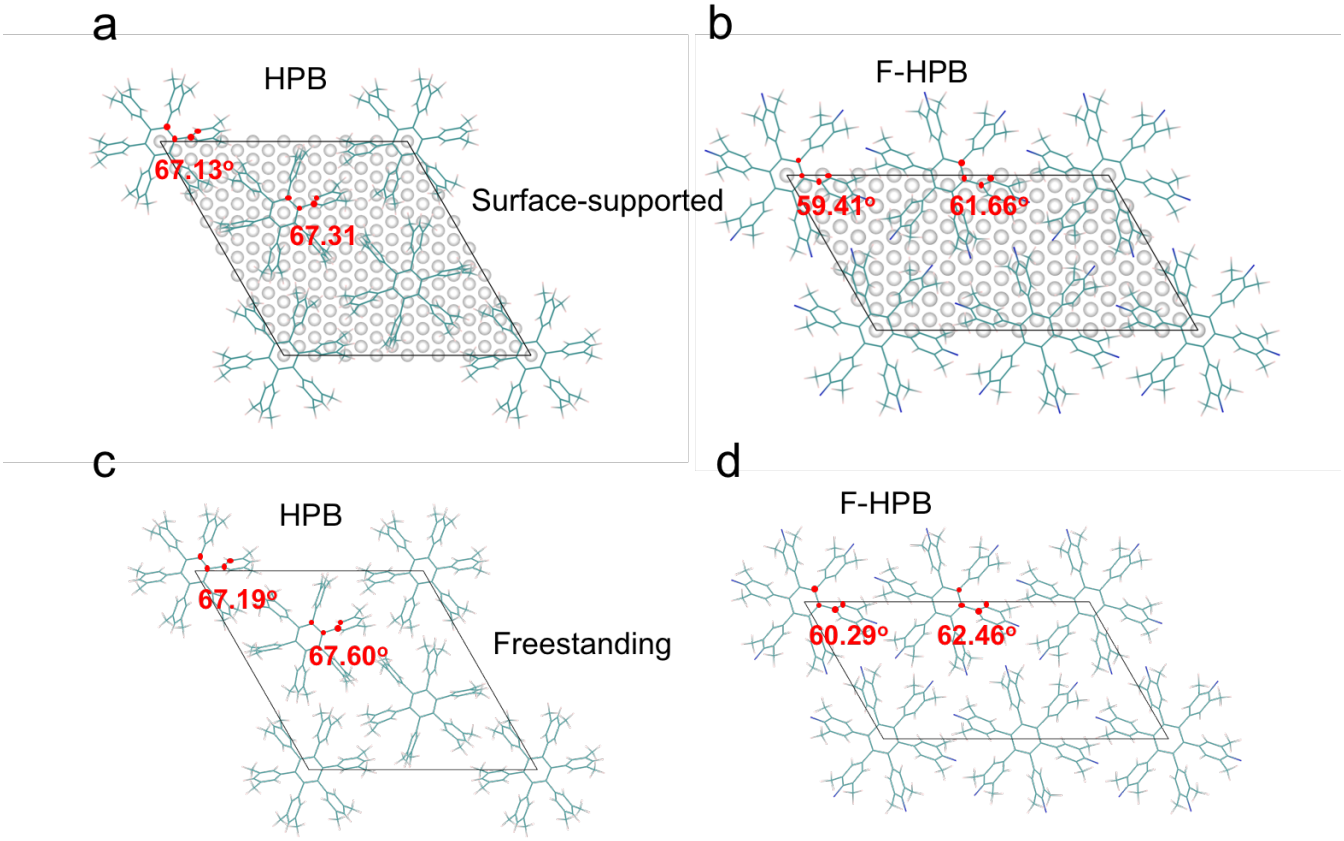

Fig. S7. (a, b) DFT-relaxed $\sqrt{3} \times \sqrt{3}$ elementary unit cell of the HPB assembly (panel a) and 2×1 unit cell of the F-HPB assembly (panel b) supported on four layers of Ag(111). (c, d) DFT-relaxed freestanding $\sqrt{3} \times \sqrt{3}$ elementary unit cell of the HPB assembly (panel c) and freestanding 2×1 unit cell of the F-HPB assembly (panel d). The values of dihedral angles are indicated on each panel.